

Energy levels, radiative rates and electron impact excitation rates for transitions in Be-like Ti XIX

Kanti M Aggarwal and Francis P Keenan

Astrophysics Research Centre, School of Mathematics and Physics, Queen's University Belfast, Belfast BT7 1NN, Northern Ireland, UK

e-mail: K.Aggarwal@qub.ac.uk

Received 23 May 2012

Accepted for publication 12 September 2012

Published xx Month 2012

Online at stacks.iop.org/PhysScr/vol/number

PACS Ref: 32.70 Cs, 34.80 Dp, 95.30 Ky

S This article has associated online supplementary data files

Tables 2 and 5 are available only in the electronic version at stacks.iop.org/PhysScr/vol/number

Abstract

We report calculations of energy levels, radiative rates and electron impact excitation cross sections and rates for transitions in Be-like Ti XIX. The GRASP (General-purpose Relativistic Atomic Structure Package) is adopted for calculating energy levels and radiative rates. For determining the collision strengths and subsequently the excitation rates, the Dirac Atomic R-matrix Code (DARC) is used. Oscillator strengths, radiative rates and line strengths are reported for all E1, E2, M1 and M2 transitions among the lowest 98 levels of the $n \leq 4$ configurations. Additionally, theoretical lifetimes are listed for all 98 levels. Collision strengths are averaged over a Maxwellian velocity distribution and the effective collision strengths obtained listed over a wide temperature range up to $10^{7.7}$ K. Comparisons are made with similar data obtained from the Flexible Atomic Code (FAC) to highlight the importance of resonances, included in calculations with DARC, in the determination of effective collision strengths. Discrepancies between the collision strengths from DARC and FAC, particularly for forbidden transitions, are also discussed.

1 Introduction

Emission lines of Ti ions, including Ti XIX, have been widely measured in laboratory plasmas [1]–[3], due to their interest for the development of x-ray lasers. Titanium is also often a material in the walls of fusion reactors, and hence many ionisation stages of this element are observed in fusion spectra due to the high temperatures. Considering its importance, several calculations have been performed in the past [4]–[9] to determine atomic data for energy levels, radiative rates (A- values), and excitation rates or equivalently the effective collision strengths (Υ), which are obtained from the electron impact collision strengths (Ω). Additionally, O’Mahony *et al* [10] have reported analytical expressions to derive values of Υ for Ti XIX, based on *R*-matrix calculations for Be-like ions between Sc XVIII and Zn XXVII. However, all these data are for transitions among the lowest 10 levels of the $n=2$ configurations of Ti XIX, and no calculation has so far been performed with the *R*-matrix code which explicitly includes the contribution of resonances in the determination of Υ . The resonance contribution to Υ may be highly significant, particularly for the forbidden transitions, as we will demonstrate in section 6. Therefore, in this work we report atomic data for energy levels, A- values, Ω and Υ for transitions among the lowest 98 levels of the $n \leq 4$ configurations of Ti XIX.

For calculations of energy levels and A-values we employ the fully relativistic GRASP (general-purpose relativistic atomic structure package) code, which was originally developed by Grant *et al* [11] and revised by Dr P H Norrington. It is a fully relativistic code, and is based on the *jj* coupling scheme. Further relativistic corrections arising from the Breit (magnetic) interaction and quantum electrodynamics (QED) effects (vacuum polarization and Lamb shift) have also been included. Additionally, we have used the option of *extended average level* (EAL), in which a weighted (proportional to $2j+1$) trace of the Hamiltonian matrix is minimized. This produces a compromise set of orbitals describing closely lying states with moderate accuracy. For our calculations of Ω , we have adopted the *Dirac Atomic R-matrix Code* (DARC) of P H Norrington and I P Grant (<http://web.am.qub.ac.uk/DARC/>). Finally, for comparison purposes, we have performed parallel calculations with the *Flexible Atomic Code* (FAC) of Gu [12], available from the website <http://sprg.ssl.berkeley.edu/~mfgu/fac/>. This is also a fully relativistic code which provides a variety of atomic parameters, and (generally) yields results for energy levels and radiative rates comparable to GRASP – see, for example, Aggarwal *et al* [13]. However, differences in collision strengths and subsequently in effective collision strengths with those obtained from DARC can be large, particularly for forbidden transitions, as demonstrated in some of our earlier papers [14]–[19], and also discussed below in sections 5 and 6. Hence results from FAC will be helpful in assessing the accuracy of our energy levels and radiative rates, and in estimating the contribution of resonances to the determination of effective collision strengths, included in calculations from DARC but not in FAC.

2 Energy levels

The 17 configurations of Ti XIX, namely $(1s^2) 2\ell 2\ell'$, $2\ell 3\ell'$ and $2\ell 4\ell'$, give rise to the lowest 98 levels listed in Table 1, where we also provide our level energies calculated from GRASP, *without* and *with* the inclusion of Breit and QED effects. Wiese and Fuhr [20] have compiled and critically evaluated experimentally measured energy levels of Ti XIX, listed at the NIST (National Institute of Standards and Technology) website <http://www.nist.gov/pml/data/asd.cfm>. These compilations are included in Table 1 for comparisons. However, NIST energies are not available for many levels, particularly of the $2\ell 4\ell'$ configurations, and for some of the levels their results are indistinguishable – see for example: 26/27 [(2p3p) 3D_2 and 1P_1] and 41/42 [2p3d $^3P_{2,1}^o$]. Also included in the table are our calculations obtained from the FAC code (FAC1), including the same CI (configuration interaction) as in GRASP.

Our level energies obtained without the Breit and QED effects (GRASP1) are higher than the NIST values by up to ~ 0.15 Ryd for some of the levels, such as: 9 ($2p^2$ 1D_2), 10 ($2p^2$ 1S_0) and 17 ($2s3d$ 3D_1). Furthermore, the ordering is also mostly the same as that of NIST. However, there are also striking differences, in both

ordering and magnitude, for some of the levels, namely 45/46 [(2p3d) $^1F_3^o$ and $^1P_1^o$], 53/54 [2s4d $^3D_{1,2}$] and 85 [2d4d $^3P_2^o$], for which the discrepancy is up to 0.4 Ryd. The inclusion of Breit and QED effects (GRASP2) lowers the energies by a maximum of ~ 0.065 Ryd, indicating that for this ion the higher relativistic effects are not too important. In addition, the ordering has slightly altered in a few instances, see for example levels 37/38 [2p3p 1D_2 and 2p3d $^3F_4^o$] and 60/61 [2s4f $^1F_3^o$ and 2p4s $^3P_0^o$]. However, the energy differences for these swapped levels are very small. Our FAC1 level energies agree with our GRASP2 calculations within 0.04 Ryd for all levels and the orderings are also the same. Small differences in the GRASP and FAC energies arise mostly by the ways calculations of central potential for radial orbitals and recoupling schemes of angular parts have been performed – see detailed discussion in the FAC manual. A further inclusion of the $2\ell 5\ell'$ configurations, labelled FAC2 calculations in Table 1, makes no appreciable difference either in the magnitude or ordering of the levels. Therefore, we are confident of our energy levels listed in Table 1, and assess these to be accurate to better than 0.5%.

3 Radiative rates

Since currently available A- values in the literature are limited to transitions among the lowest 10 levels of Ti XIX, we here provide a complete set of data for all transitions among the 98 levels and for four types, namely electric dipole (E1), electric quadrupole (E2), magnetic dipole (M1), and magnetic quadrupole (M2), as these are required in a plasma model. Furthermore, the absorption oscillator strength (f_{ij}) and radiative rate A_{ji} (in s^{-1}) for a transition $i \rightarrow j$ are related by the following expression [21]:

$$f_{ij} = \frac{mc}{8\pi^2 e^2} \lambda_{ji}^2 \frac{\omega_j}{\omega_i} A_{ji} = 1.49 \times 10^{-16} \lambda_{ji}^2 (\omega_j/\omega_i) A_{ji} \quad (1)$$

where m and e are the electron mass and charge, respectively, c is the velocity of light, λ_{ji} is the transition energy/wavelength in \AA , and ω_i and ω_j are the statistical weights of the lower (i) and upper (j) levels, respectively. Similarly, the oscillator strength f_{ij} (dimensionless) and the line strength S (in atomic unit, 1 a.u. = 6.460×10^{-36} cm² esu²) are related by the standard equations given below [21]-[23].

For the electric dipole (E1) transitions

$$A_{ji} = \frac{2.0261 \times 10^{18}}{\omega_j \lambda_{ji}^3} S^{E1} \quad \text{and} \quad f_{ij} = \frac{303.75}{\lambda_{ji} \omega_i} S^{E1}, \quad (2)$$

for the magnetic dipole (M1) transitions

$$A_{ji} = \frac{2.6974 \times 10^{13}}{\omega_j \lambda_{ji}^3} S^{M1} \quad \text{and} \quad f_{ij} = \frac{4.044 \times 10^{-3}}{\lambda_{ji} \omega_i} S^{M1}, \quad (3)$$

for the electric quadrupole (E2) transitions

$$A_{ji} = \frac{1.1199 \times 10^{18}}{\omega_j \lambda_{ji}^5} S^{E2} \quad \text{and} \quad f_{ij} = \frac{167.89}{\lambda_{ji}^3 \omega_i} S^{E2}, \quad (4)$$

and for the magnetic quadrupole (M2) transitions

$$A_{ji} = \frac{1.4910 \times 10^{13}}{\omega_j \lambda_{ji}^5} S^{M2} \quad \text{and} \quad f_{ij} = \frac{2.236 \times 10^{-3}}{\lambda_{ji}^3 \omega_i} S^{M2}. \quad (5)$$

In Table 2 we present transition energies/wavelengths (λ , in \AA), radiative rates (A_{ji} , in s^{-1}), oscillator strengths (f_{ij} , dimensionless), and line strengths (S , in a.u.), in length form only, for all 1468 electric dipole (E1) transitions among the 98 levels of Ti XIX. The *indices* used to represent the lower and upper levels of a transition have already been defined in Table 1. Similarly, there are 1754 electric quadrupole (E2), 1424 magnetic dipole (M1), and 1792 magnetic quadrupole (M2) transitions among the 98 levels. However, for

these transitions only the A-values are listed in Table 2, and the corresponding results for f- or S- values can be easily obtained using Eqs. (1–5).

As noted earlier, A-values in the literature for Ti XIX are only available for a limited number of transitions. Therefore, we have performed another calculation with the FAC code of Gu [12]. In Table 3 we compare our A- values from both the GRASP and FAC codes for some transitions among the lowest 20 levels of Ti XIX. Also included in this table are f- values from GRASP because they give an indication of the strength of a transition. Similarly, to facilitate easy comparison between the two calculations, we have also listed the ratio of A-values obtained with the GRASP and FAC codes. For these (and many other) transitions, the agreement between the two sets of A- values is better than 20%. Indeed, for most strong transitions ($f \geq 0.01$), the A-values from GRASP and FAC agree to better than 20%, and the only exceptions are three transitions, namely 2–32 ($2s2p\ ^3P_0^o - 2p3p\ ^3S_1$), 32–71 ($2p3p\ ^3S_1 - 2p4d\ ^3D_2^o$) and 32–83 ($2p3p\ ^3S_1 - 2p4d\ ^1D_2^o$), for which the discrepancies are up to 40%. These discrepancies mainly arise from the corresponding differences in the energy levels. Furthermore, for a majority (80%) of the strong E1 transitions ($f \geq 0.01$) the length and velocity forms in our GRASP calculations agree within 20%, and discrepancies for the others are mostly within a factor of two. However, for a few ($\sim 13\%$) weaker transitions ($f \leq 10^{-3}$) the two forms of the f- value differ by up to several orders of magnitude, and examples include: 4–24 ($f \sim 3 \times 10^{-10}$), 4–92 ($f \sim 4 \times 10^{-7}$), 29–31 ($f \sim 5 \times 10^{-9}$), 30–31 ($f \sim 6 \times 10^{-7}$) and 33–34 ($f \sim 3 \times 10^{-6}$). Finally, as for the energy levels, the effect of additional CI is negligible on the A- values, as results for all strong E1 transitions agree within $\sim 20\%$ with those obtained with the inclusion of the $n = 5$ configurations. To conclude, we may state that for almost all strong E1 transitions, our radiative rates are accurate to better than 20%. However, for the weaker transitions the accuracy is comparatively poorer.

4 Lifetimes

The lifetime τ for a level j is defined as follows [24]:

$$\tau_j = \frac{1}{\sum_i A_{ji}}. \quad (6)$$

Since this is a measurable parameter, it provides a check on the accuracy of the calculations. Therefore, in Table 1 we have also listed our calculated lifetimes, which include the contributions from four types of transitions, i.e. E1, E2, M1, and M2. To our knowledge, no calculations or measurements are available for lifetimes for any of the Ti XIX levels. However, we hope the present results will be useful for future comparisons and may encourage experimentalists to measure lifetimes, particularly for the level $2s2p\ ^3P_2^o$ which has a comparatively large value of ~ 1 ms.

5 Collision strengths

Collision strengths (Ω) are related to the more commonly known parameter collision cross section (σ_{ij} , πa_0^2) by the following relationship [25]:

$$\Omega_{ij}(E) = k_i^2 \omega_i \sigma_{ij}(E) \quad (7)$$

where k_i^2 is the incident energy of the electron and ω_i is the statistical weight of the initial state. Results for collisional data are preferred in the form of Ω because it is a symmetric and dimensionless quantity.

For the computation of collision strengths Ω , we have employed the *Dirac atomic R-matrix code* (DARC), which includes the relativistic effects in a systematic way, in both the target description and the scattering model. It is based on the jj coupling scheme, and uses the Dirac-Coulomb Hamiltonian in the R -matrix approach. The R -matrix radius adopted for Ti XIX is 3.64 au, and 55 continuum orbitals have been included for each channel angular momentum in the expansion of the wavefunction, allowing us to compute Ω up to

an energy of 1150 Ryd, i.e. ~ 1070 Ryd *above* the highest threshold, equivalent to $\sim 1.7 \times 10^8$ K. This energy range is sufficient to calculate values of effective collision strength Υ (see section 6) up to $T_e = 10^{7.7}$ K, well above the temperature of maximum abundance in ionisation equilibrium for Ti XIX, i.e. $10^{6.9}$ K [26]. The maximum number of channels for a partial wave is 428, and the corresponding size of the Hamiltonian matrix is 23 579. To obtain convergence of Ω for all transitions and at all energies, we have included all partial waves with angular momentum $J \leq 40.5$, although a larger number would have been preferable for the convergence of some allowed transitions, especially at higher energies. However, to account for higher neglected partial waves, we have included a top-up, based on the Coulomb-Bethe approximation [27] for allowed transitions and geometric series for others.

For illustration, in Figs. 1-3 we show the variation of Ω with angular momentum J for three transitions of Ti XIX, namely 1-5 ($2s^2 \ ^1S_0 - 2s2p \ ^1P_1^o$), 2-4 ($2s2p \ ^3P_0^o - 2s2p \ ^3P_2^o$) and 9-10 ($2p^2 \ ^1D_0 - 2p^2 \ ^1S_0$), and at three energies of 100, 500 and 900 Ryd. The values of Ω have not converged for allowed transitions as shown in Fig. 1, for which a top-up has been included as mentioned above, and has been found to be appreciable. However, for all forbidden transitions, the values of Ω have fully converged as shown in Figs. 2 and 3. It is also clear from Figs. 2 and 3 that a large range of partial waves is required for the convergence of Ω for some of the forbidden transitions, particularly towards the higher end of the energy range.

In Table 4 we list our values of Ω for resonance transitions of Ti XIX at energies *above* thresholds. The indices used to represent the levels of a transition have already been defined in Table 1. Unfortunately, no similar data are available for comparison purposes as already noted in section 1. Therefore, to make an accuracy assessment for Ω , we have performed another calculation using the FAC code of Gu [12]. This code is also fully relativistic, and is based on the well-known and widely-used *distorted-wave* (DW) method – see for example, [28]–[29] and the FAC manual. Furthermore, the same CI is included in FAC as in the calculations from DARC. Therefore, also included in Table 4 for comparison purposes are the Ω values from FAC at a single *excited* energy E_j , which corresponds to an incident energy of ~ 700 Ryd for Ti XIX. For $\sim 60\%$ of the Ti XIX transitions, the values of Ω with the DARC and FAC codes agree within 20% at an energy of 700 Ryd. However, the discrepancies for others are much higher, particularly for weaker transitions, such as: 1-30/31/35/39/73/77/83/89/91. Most of these are weak ($\Omega \leq 10^{-6}$) and forbidden, i.e. the values of Ω have fully converged at *all* energies within our adopted range of partial waves in the calculations with the DARC code. For such weak transitions, values of Ω from the FAC code are not assessed to be accurate. Additionally, for a few transitions, such as 49-87, 50-72/86/98, 51-66/69/71/83/85, 52-68/72/86/98 and 53-63/64/77/95, the values of Ω from the FAC code show a sudden increase, by orders of magnitude at some random energies, generally towards the higher end. This problem is common for many ions and examples of this can be seen in Fig. 6 of Aggarwal and Keenan [17], [18]. The sudden anomalous behaviour in Ω with the FAC code is also responsible for the differences noted above for many transitions. Such anomalies for some transitions (both allowed and forbidden) from the FAC calculations arise primarily because of the interpolation and extrapolation techniques employed in the code. In order to expedite calculations, i.e. to generate a large amount of atomic data in a comparatively very short period of time, and without too large loss of accuracy, calculations of Ω are not performed at each partial wave, but only at each J up to 5, and then the interval between successive calculations is doubled every two points, i.e. the grid is almost logarithmic – see the FAC manual for further details. Similarly, some differences in Ω are expected because the DW method generally overestimates results due to the exclusion of channel coupling.

As a further comparison between the DARC and FAC values of Ω , in Fig. 4 we show the variation of Ω with energy for three *allowed* transitions among the excited levels of Ti XIX, namely 4-19 ($2s2p \ ^3P_2^o - 2s3d \ ^3D_3$), 5-20 ($2s2p \ ^1P_1^o - 2s3d \ ^1D_2$), and 8-40 ($2p^2 \ ^3P_2 - 2p3d \ ^3D_3^o$). For many transitions there are no discrepancies between the f -values obtained with the two different codes (GRASP and FAC) as demonstrated in Table 3, and therefore the values of Ω also agree to better than 20%. Similar comparisons between the two calculations with DARC and FAC are shown in Fig. 5 for three *forbidden* transitions of Ti XIX, namely 1-12 ($2s^2 \ ^1S_0 - 2s3s \ ^1S_0$), 2-4 ($2s2p \ ^3P_0^o - 2s2p \ ^3P_2^o$), and 3-4 ($2s2p \ ^3P_1^o - 2s2p \ ^3P_2^o$). As in the case of the allowed transitions,

for these forbidden ones the agreement between the two calculations is generally satisfactory, although there are some differences towards the lower end of the energy range. Therefore, on the basis of these and other comparisons discussed above, collision strengths from our DARC code are assessed to be accurate to better than 20%. However, similar data from FAC are not assessed to be accurate for all transitions over an entire energy range.

6 Effective collision strengths

Excitation rates, in addition to energy levels and radiative rates, are required for plasma modelling, and are determined from the collision strengths (Ω). Since the threshold energy region is dominated by numerous closed-channel (Feshbach) resonances, values of Ω need to be calculated in a fine energy mesh to accurately account for their contribution. Furthermore, in a plasma electrons have a wide distribution of velocities, and therefore values of Ω are generally averaged over a *Maxwellian* distribution as follows [25]:

$$\Upsilon(T_e) = \int_0^\infty \Omega(E) \exp(-E_j/kT_e) d(E_j/kT_e), \quad (8)$$

where k is Boltzmann constant, T_e electron temperature in K, and E_j the electron energy with respect to the final (excited) state. Once the value of Υ is known the corresponding results for the excitation $q(i,j)$ and de-excitation $q(j,i)$ rates can be easily obtained from the following equations:

$$q(i,j) = \frac{8.63 \times 10^{-6}}{\omega_i T_e^{1/2}} \Upsilon \exp(-E_{ij}/kT_e) \quad \text{cm}^3 \text{s}^{-1} \quad (9)$$

and

$$q(j,i) = \frac{8.63 \times 10^{-6}}{\omega_j T_e^{1/2}} \Upsilon \quad \text{cm}^3 \text{s}^{-1}, \quad (10)$$

where ω_i and ω_j are the statistical weights of the initial (i) and final (j) states, respectively, and E_{ij} is the transition energy. The contribution of resonances may enhance the values of Υ over those of the background collision strengths (Ω_B), especially for the forbidden transitions, by up to an order of magnitude (or even more) depending on the transition and/or the temperature. Similarly, values of Ω need to be calculated over a wide energy range (above thresholds) to obtain convergence of the integral in Eq. (8), as demonstrated in Fig. 7 of Aggarwal and Keenan [30]. It may be noted that if for practical reasons calculations of Ω are performed only up to a limited range of energy then the high energy limits for a range of transitions can be invoked through the expressions suggested by Burgess and Tully [25]. However, there is no such need in the present work as calculations for Ω have been performed up to a reasonably high energy range, as noted in section 5.

To delineate resonances, we have performed our calculations of Ω at over $\sim 41\,000$ energies in the thresholds region. Close to thresholds (~ 0.1 Ryd above a threshold) the energy mesh is 0.001 Ryd, and away from thresholds is 0.002 Ryd. Hence care has been taken to include as many resonances as possible, and with as fine a resolution as is computationally feasible. The density and importance of resonances can be appreciated from Figs. 6–11, where we plot Ω as a function of energy in the thresholds region for the 1–2 ($2s^2 \ ^1S_0 - 2s2p \ ^3P_0^o$), 1–3 ($2s^2 \ ^1S_0 - 2s2p \ ^3P_1^o$), 1–4 ($2s^2 \ ^1S_0 - 2s2p \ ^3P_2^o$), 2–3 ($2s2p \ ^3P_0^o - 2s2p \ ^3P_1^o$), 2–4 ($2s2p \ ^3P_0^o - 2s2p \ ^3P_2^o$) and 3–4 ($2s2p \ ^3P_1^o - 2s2p \ ^3P_2^o$) transitions, respectively. For all these (and many other) transitions the resonances are dense over the entire thresholds energy range, and hence make a significant contribution to Υ over a wide range of temperatures. Since for many transitions, resonances are dense and have high magnitude at energies close to the thresholds, a slight displacement in their positions can significantly affect the calculations of Υ , mostly at the low temperatures, but not at the higher ones required for Ti XIX.

Our calculated values of Υ are listed in Table 5 over a wide temperature range up to $10^{7.7}$ K, suitable for applications to a variety of plasmas. Corresponding data at any other temperature/s and/or in a different format in a machine readable form can also be requested from any one of the authors. As stated in section

1, there are only limited results available for comparison purposes. Therefore, we have also calculated values of Υ from our non-resonant Ω data obtained with the FAC code, and these are included at the lowest and the highest calculated temperatures. These calculations are particularly helpful in providing an estimate of the importance of resonances in the determination of excitation rates. Furthermore, Zhang and Sampson [7] (ZS) have reported values of Υ for transitions among the lowest 10 levels of Ti XIX. In their calculations, they have adopted the Coulomb-Born-Exchange method and their results are stored in the CHIANTI database at http://www.chiantidatabase.org/chianti_direct_data.html. In Table 6 we compare our results for Υ , from both DARC and FAC, with those of ZS at three temperatures of $10^{6.3}$, $10^{6.9}$ and $10^{7.5}$ K. Values of Υ from FAC generally agree with those of ZS within 20%, because both calculations are based on the DW method and do not include the contribution of resonances. However, our corresponding results from DARC are higher, by up to a factor of four, for many transitions, mostly forbidden. This is because of the inclusion of resonances in the calculations with DARC. Moreover, since resonances are spread over a wide energy range, as noted in Figs. 6–11, higher values of Υ are sustained over the entire range of temperatures over which the calculations have been performed – see for example transitions 1–2/4/6/7/8/9/10.

The comparison of Υ in Table 6 is limited to the 45 transitions among the lowest 10 levels of Ti XIX. For a larger range of transitions, about half have a discrepancy of more than 20% over the entire range of temperatures. At lower temperatures, the differences are generally within a factor of 5, but are higher (up to two orders of magnitude) for some, such as: 2–38 ($2s2p\ ^3P_0^o - 2p3d\ ^3F_4^o$), 6–11 ($2p^2\ ^3P_0 - 2s3s\ ^3S_1$), 7–11 ($2p^2\ ^3P_1 - 2s3s\ ^3S_1$), 8–11 ($2p^2\ ^3P_2 - 2s3s\ ^3S_1$) and 9–51 ($2p^2\ ^1D_2 - 2s4p\ ^3P_2^o$). Similarly, towards higher temperatures, the discrepancies for most transitions are within a factor of two, but are larger by up to orders of magnitude for a few, such as: 2–38/43, 6–11/14/16/17 and 7–11/18/19. In most cases, our results from DARC are higher because of the inclusion of resonances. However, in a few cases the values of Υ from FAC are abnormally greater because of the anomaly in the calculated values of Ω , as discussed in section 5.

7 Conclusions

In this paper we have presented results for energy levels and radiative rates for four types of transitions (E1, E2, M1, and M2) among the lowest 98 levels of Ti XIX belonging to the $n \leq 4$ configurations. Additionally, lifetimes of all the calculated levels have been reported, although no measurements or other theoretical results are available for comparison. However, based on a variety of comparisons among various calculations with the GRASP and FAC codes, our results for radiative rates, oscillator strengths, line strengths, lifetimes and collision strengths are judged to be accurate to better than 20% for a majority of the strong transitions (levels). Furthermore, for calculations of Υ , resonances in the thresholds energy region are noted to be dominant for many transitions, and inclusion of their contribution has significantly enhanced the results. In the absence of other similar calculations, it is difficult to fully assess the accuracy of our Υ results. However, since we have considered a large range of partial waves to achieve convergence of Ω at all energies, included a wide energy range to calculate values of Υ up to $T_e = 10^{7.7}$ K, and resolved resonances in a fine energy mesh to account for their contributions, we see no apparent deficiency in our reported data. Therefore, based on the comparisons made in section 6 and our past experience with calculations on other ions, we estimate the accuracy of our results for Υ to be better than 20% for most transitions. Nevertheless, the present data for Υ for transitions involving the levels of the $n = 4$ configurations may perhaps be improved by the inclusion of the levels of the $n = 5$ configurations. Furthermore, for some highly charged ions, particularly He-like, the effect of radiation damping may reduce the contribution of resonances in the determination of effective collision strengths. While this may be true for a few transitions towards the lower end of the temperature range, as demonstrated by several workers, see for example: [31]–[33], the effect is not appreciable at high temperatures at which data are applied in the modelling of plasmas, as discussed in some of our earlier papers, such as: [17]–[19] and [34]. Nevertheless, scope remains for improvement in the reported data but until then we believe the present set of complete results for radiative and excitation rates for transitions in Ti XIX will be highly useful for the

modelling of a variety of plasmas.

References

- [1] Goldsmith S, Oren L, Crooker A M and Cohen L 1973 *Astrophys. J.* **184** 1021
- [2] Moreno J C, Goldsmith S, Griem H R, Cohen L and Richardson M C 1987 *J. Opt. Soc. Am.* **B4** 1931
- [3] Zhihu Y, Shubin D U, Hong S U, Yanping Z, Shouting R and Xiantang Z 2004 *Chinese Sci. Bulletin* **49** 2443
- [4] Bhatia A K, Feldman U and Doschek G A 1980 *J. Appl. Phys.* **51** 1464
- [5] Bhatia AK, Feldman U and Seely J F 1986 *At. Data Nucl. Data Tables* **35** 449
- [6] Sampson DH, Goett S J and Clark R E H 1984 *At. Data Nucl. Data Tables* **30** 125
- [7] Zhang H and Sampson D H 1992 *At. Data Nucl. Data Tables* **52** 143
- [8] Clark R E H and Abdallah J 1991 *Phys. Scr.* **T37** 28
- [9] Farrag A 2006 *Elect. J. Theort. Phys.* **3** 111
- [10] O'Mahony N, Keenan F P and Conlon E S 1994 *Phys. Scr.* **49** 675
- [11] Grant I P, McKenzie B J, Norrington P H, Mayers D F and Pyper N C 1980 *Comput. Phys. Commun.* **21** 207
- [12] Gu M F 2008 *Can. J. Phys.* **86** 675
- [13] Aggarwal K M, Tayal V, Gupta G P and Keenan F P 2007 *At. Data Nucl. Data Tables* **93** 615
- [14] Aggarwal K M, Keenan F P and Heeter R F 2009 *Phys. Scr.* **80** 045301
- [15] Aggarwal K M and Keenan F P 2010 *Phys. Scr.* **82** 065302
- [16] Aggarwal K M, Kato T, Keenan F P and Murakami I 2011 *Phys. Scr.* **83** 015302
- [17] Aggarwal K M and Keenan F P 2012a *Phys. Scr.* **85** 025305
- [18] Aggarwal K M and Keenan F P 2012b *Phys. Scr.* **85** 025306
- [19] Aggarwal K M and Keenan F P 2012c *Phys. Scr.* **85** 065301
- [20] Wiese W L and Fuhr J R 1975 *J. Phys. Chem. Ref. Data* **4** 263
- [21] Garstang R H 1968 *J. Phys.* **B1** 847
- [22] Shore B W and Menzel D H 1968 *Principles of Atomic Spectra*, New York: Wiley
- [23] Safronova U I, Namba C, Murakami I, Johnson W R and Safronova M S 2001 *Phys. Rev.* **A64** 012507
- [24] Woodgate G K 1970 *Elementary Atomic Structure*, New York: McGraw-Hill
- [25] Burgess A and Tully J A 1992 *Astron. Astrophys.* **254** 436
- [26] Bryans P, Landi E and Savin D W 2009 *Astrophys. J.* **691** 1540
- [27] Burgess A and Sheorey V B 1974 *J. Phys.* **B7** 2403
- [28] Eissner W and Seaton M J 1972 *J. Phys.* **B5** 2187

- [29] Eissner 1998 *Comput. Phys. Commun.* **114** 295
- [30] Aggarwal K M and Keenan F P 2008 *Eur. Phys. J. D* **46** 205
- [31] Delahaye F, Pradhan A K and Zeippen C J 2006 *J. Phys.* **B39** 3465
- [32] Whiteford A D, Badnell N R, Ballance C P, O'Mullane M G, Summers H P and Thomas A L 2001 *J. Phys.* **B 34** 3179
- [33] Griffin D C and Ballance C P 2009 *J. Phys.* **B 42** 235201
- [34] Aggarwal K M and Keenan F P 2012d *Phys. Scr.* **86** in press

Figure 1. Partial collision strengths for the 1–5 transition of Ti XIX.

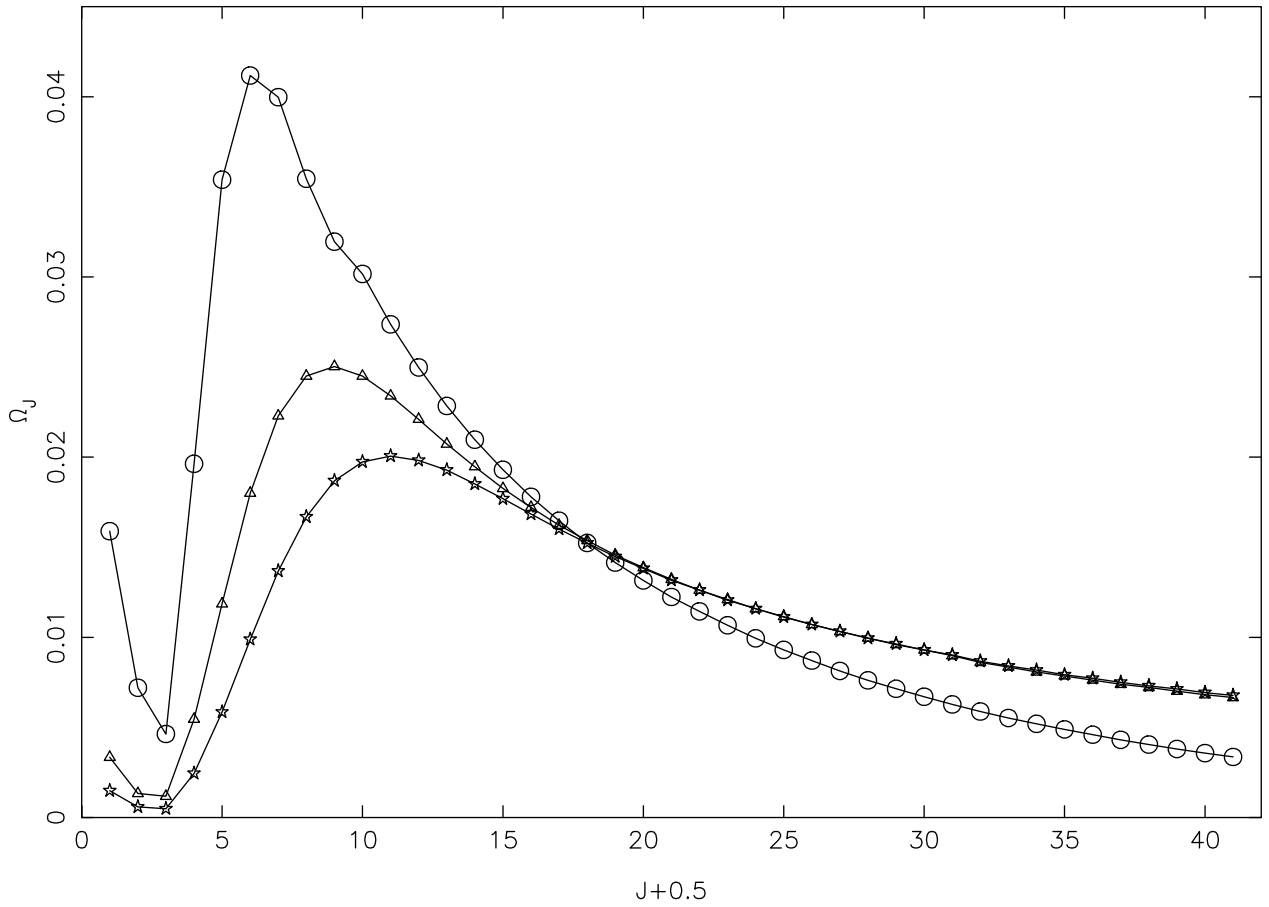


Figure 1: Partial collision strengths for the $2s^2\ ^1S_0 - 2s2p\ ^1P_1^o$ (1–5) transition of Ti XIX, at three energies of: 100 Ryd (circles), 500 Ryd (triangles) and 900 Ryd (stars).

Figure 2. Partial collision strengths for the 2–4 transition of Ti XIX.

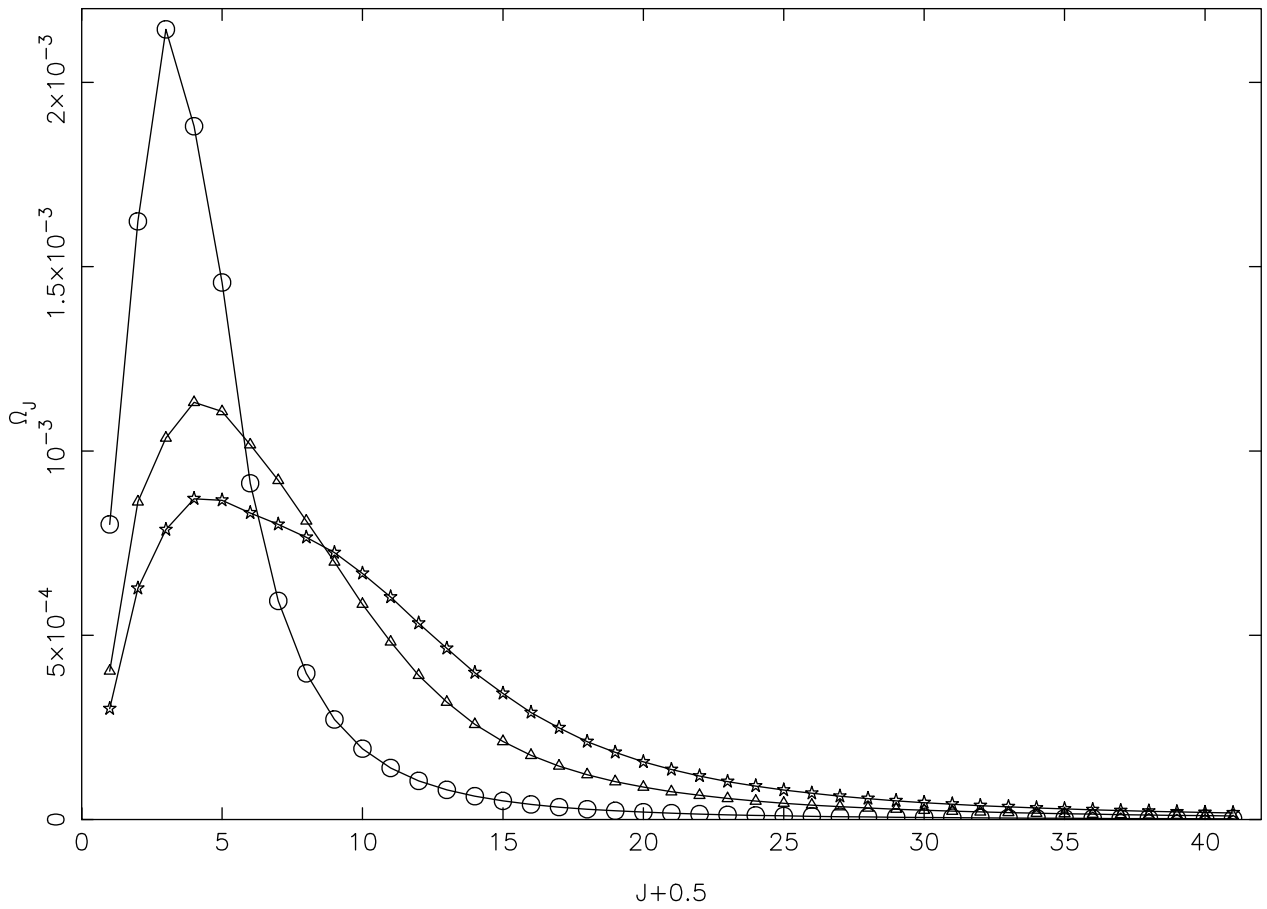


Figure 2: Partial collision strengths for the $2s2p \ ^3P_0^o - 2s2p \ ^3P_2^o$ (2–4) transition of Ti XIX, at three energies of: 100 Ryd (circles), 500 Ryd (triangles) and 900 Ryd (stars).

Figure 3. Partial collision strengths for the 9–10 transition of Ti XIX.

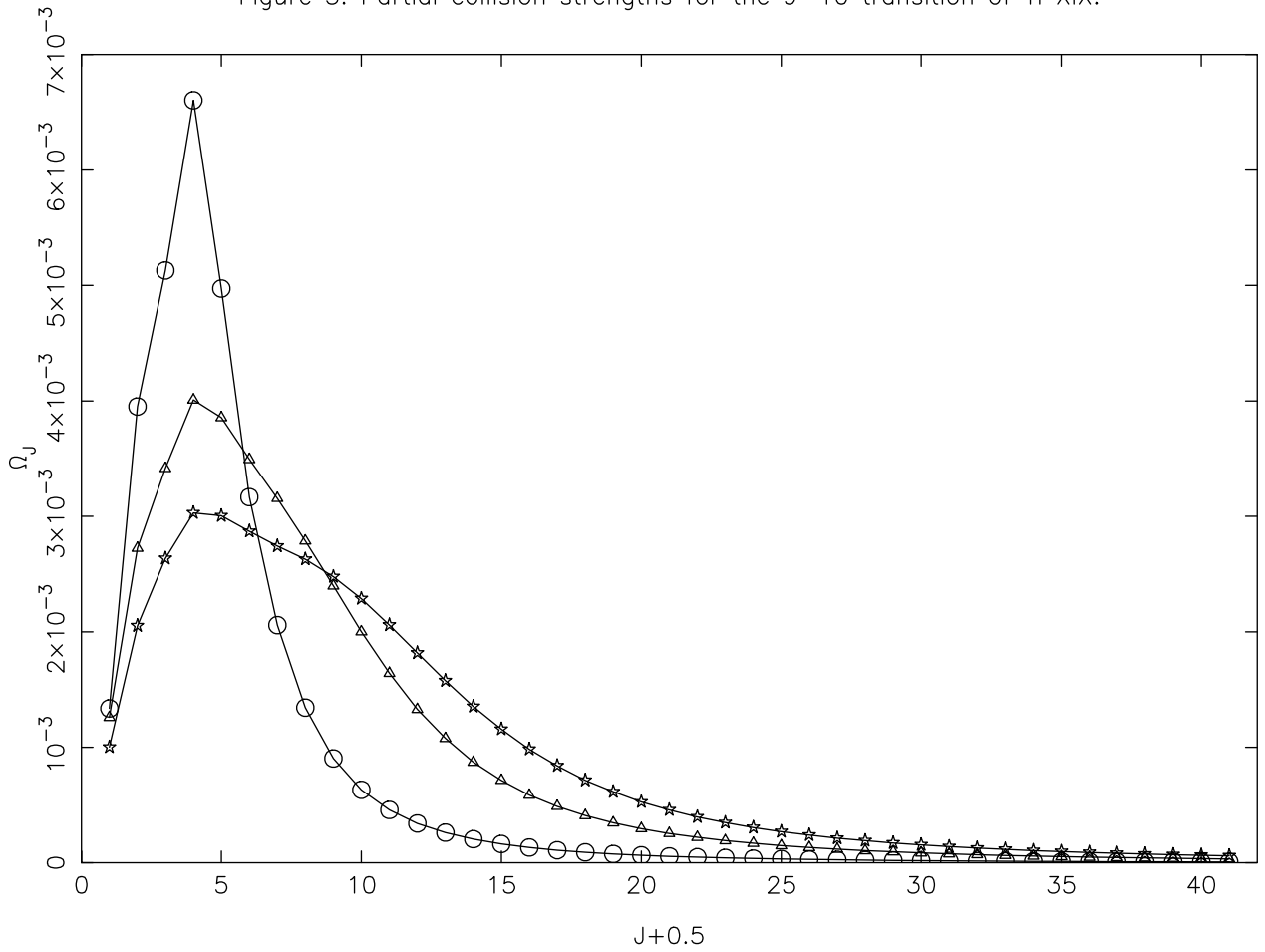


Figure 3: Partial collision strengths for the $2p^2 \ ^1D_0 - 2p^2 \ ^1S_0$ (9–10) transition of Ti XIX, at three energies of: 100 Ryd (circles), 500 Ryd (triangles) and 900 Ryd (stars).

Figure 4. Comparison of collision strengths for the 4–19, 5–20, and 8–40 allowed transitions of Ti XIX.

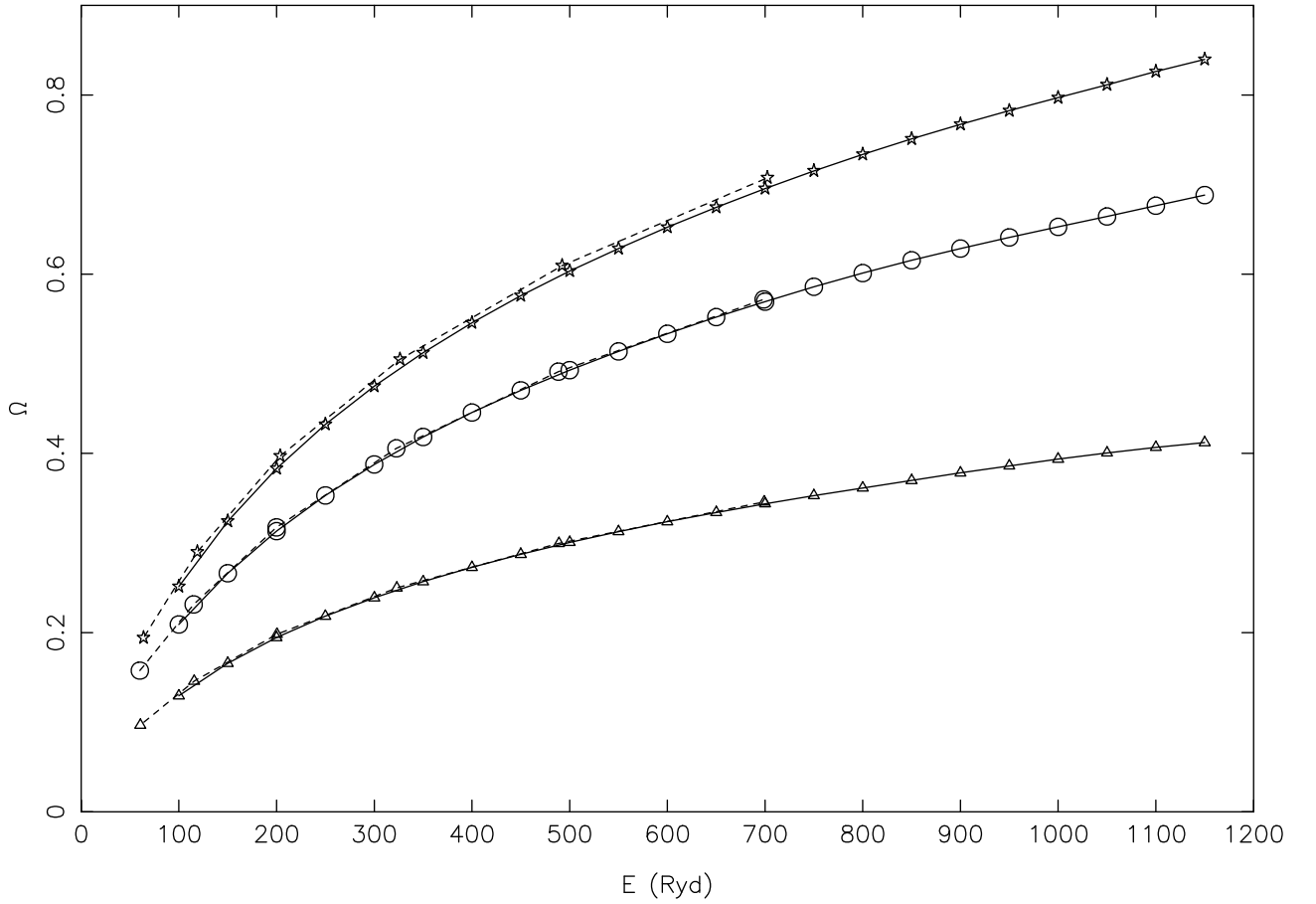


Figure 4: Comparison of collision strengths from our calculations from DARC (continuous curves) and FAC (broken curves) for the 4–19 (circles: $2s2p\ ^3P_2^o - 2s3d\ ^3D_3$), 5–20 (triangles: $2s2p\ ^1P_1^o - 2s3d\ ^1D_2$), and 8–40 (stars: $2p^2\ ^3P_2 - 2p3d\ ^3D_3^o$) allowed transitions of Ti XIX.

Figure 5. Comparison of collision strengths for the 1–12, 2–4, and 3–4 forbidden transitions of Ti XIX.

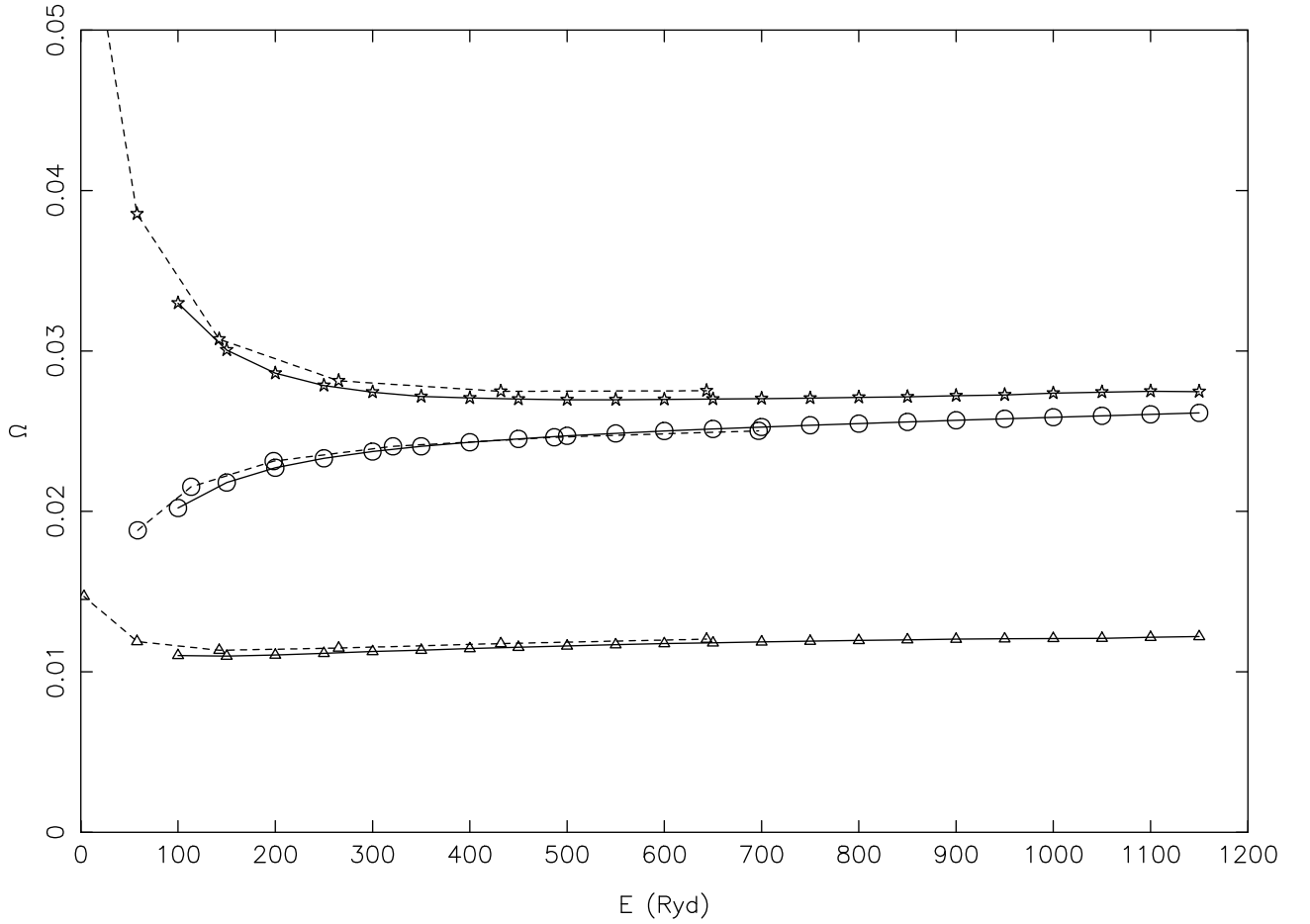


Figure 5: Comparison of collision strengths from our calculations from DARC (continuous curves) and FAC (broken curves) for the 1–12 (circles: $2s^2\ ^1S_0 - 2s3s\ ^1S_0$), 2–4 (triangles: $2s2p\ ^3P_0^o - 2s2p\ ^3P_2^o$), and 3–4 (stars: $2s2p\ ^3P_1^o - 2s2p\ ^3P_2^o$) forbidden transitions of Ti XIX.

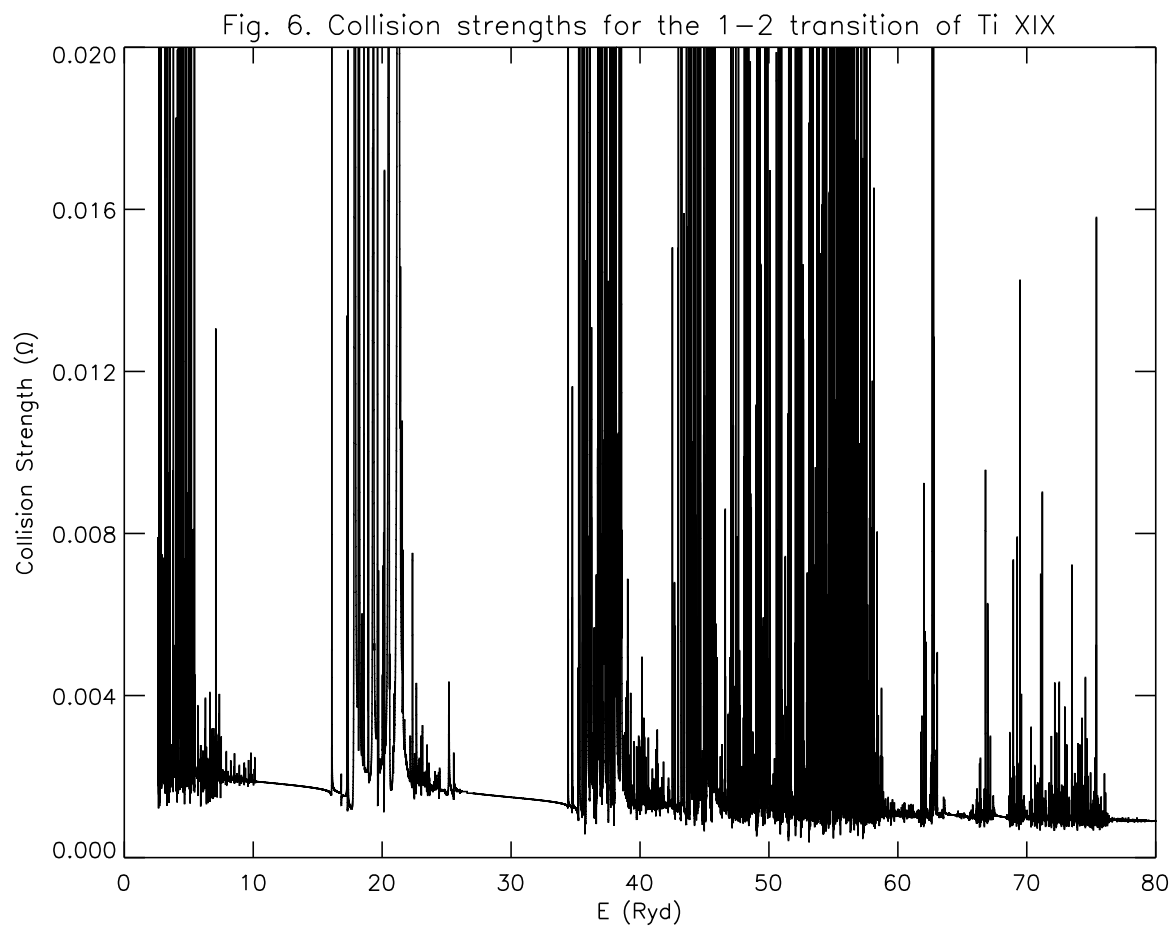


Figure 6: Collision strengths for the $2s^2\ ^1S_0 - 2s2p\ ^3P_0^o$ (1–2) transition of Ti XIX.

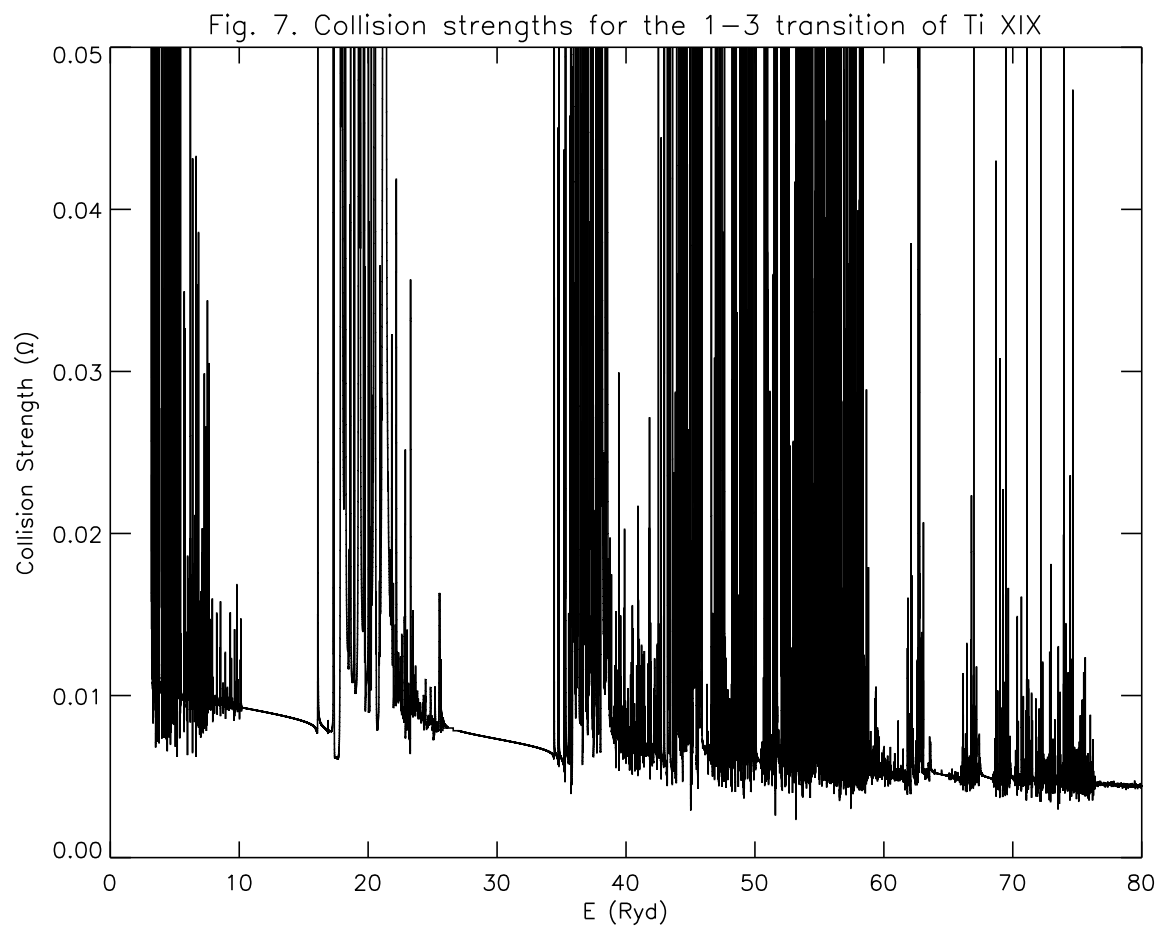


Figure 7: Collision strengths for the $2s^2\ ^1S_0 - 2s2p\ ^3P_1^o$ (1–3) transition of Ti XIX.

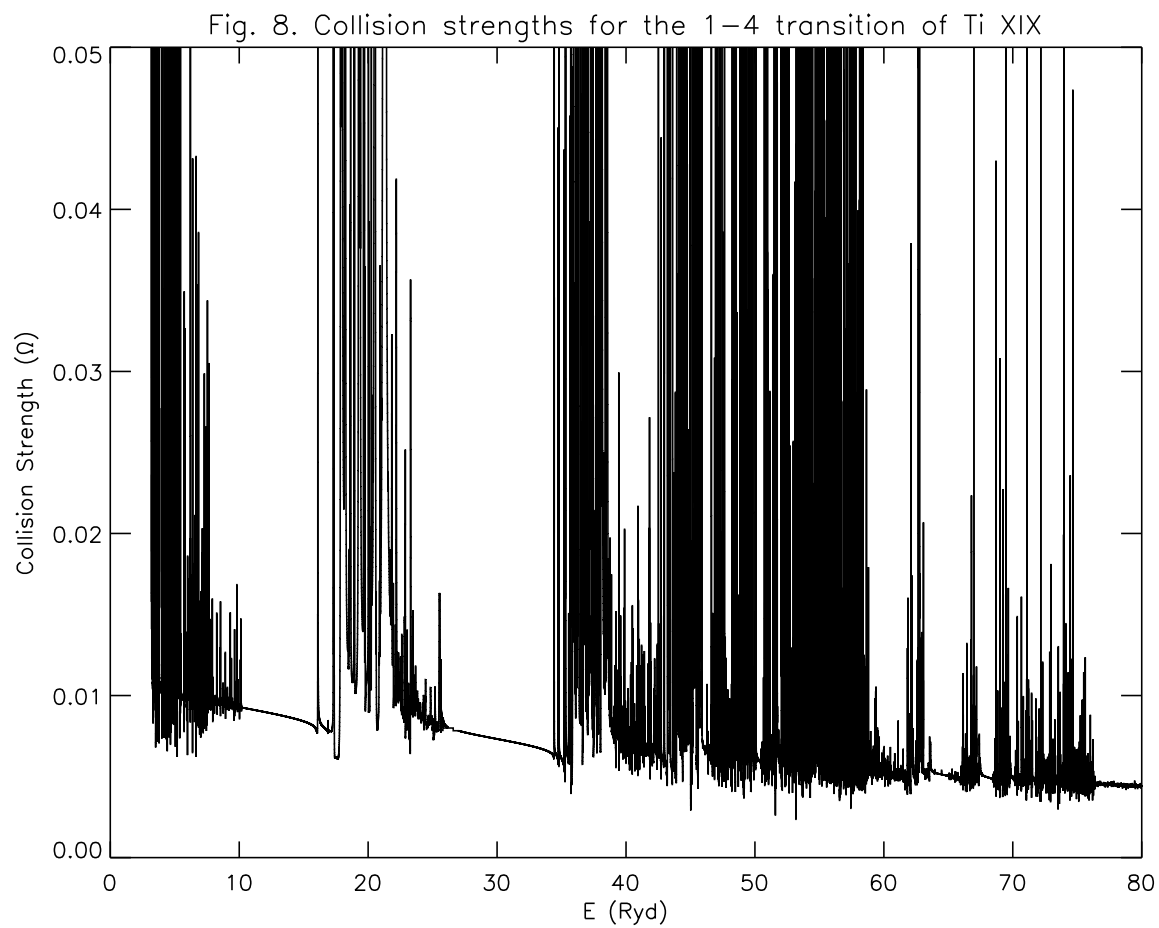


Figure 8: Collision strengths for the $2s^2\ ^1S_0 - 2s2p\ ^3P_2^o$ (1–4) transition of Ti XIX.

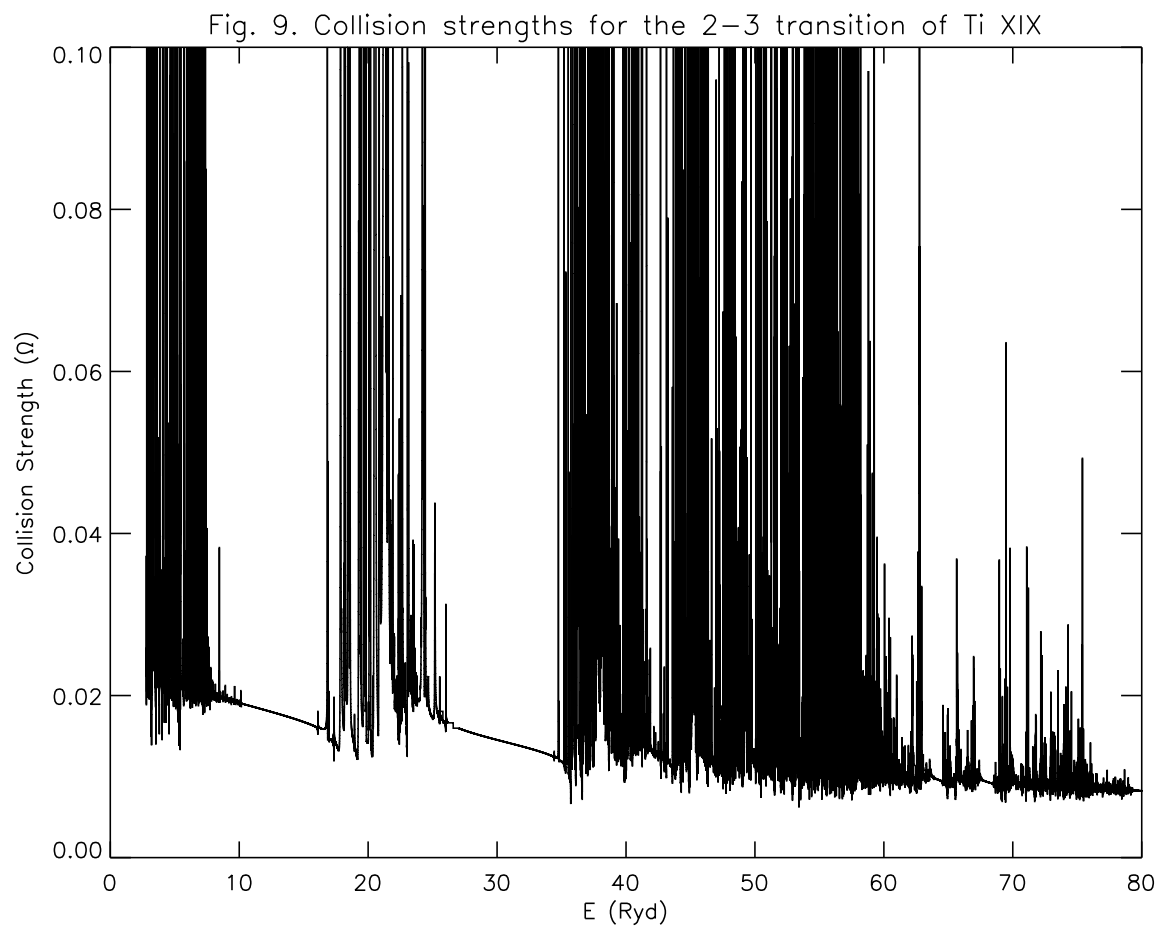


Figure 9: Collision strengths for the $2s2p\ ^3P_0^o - 2s2p\ ^3P_1^o$ (2–3) transition of Ti XIX.

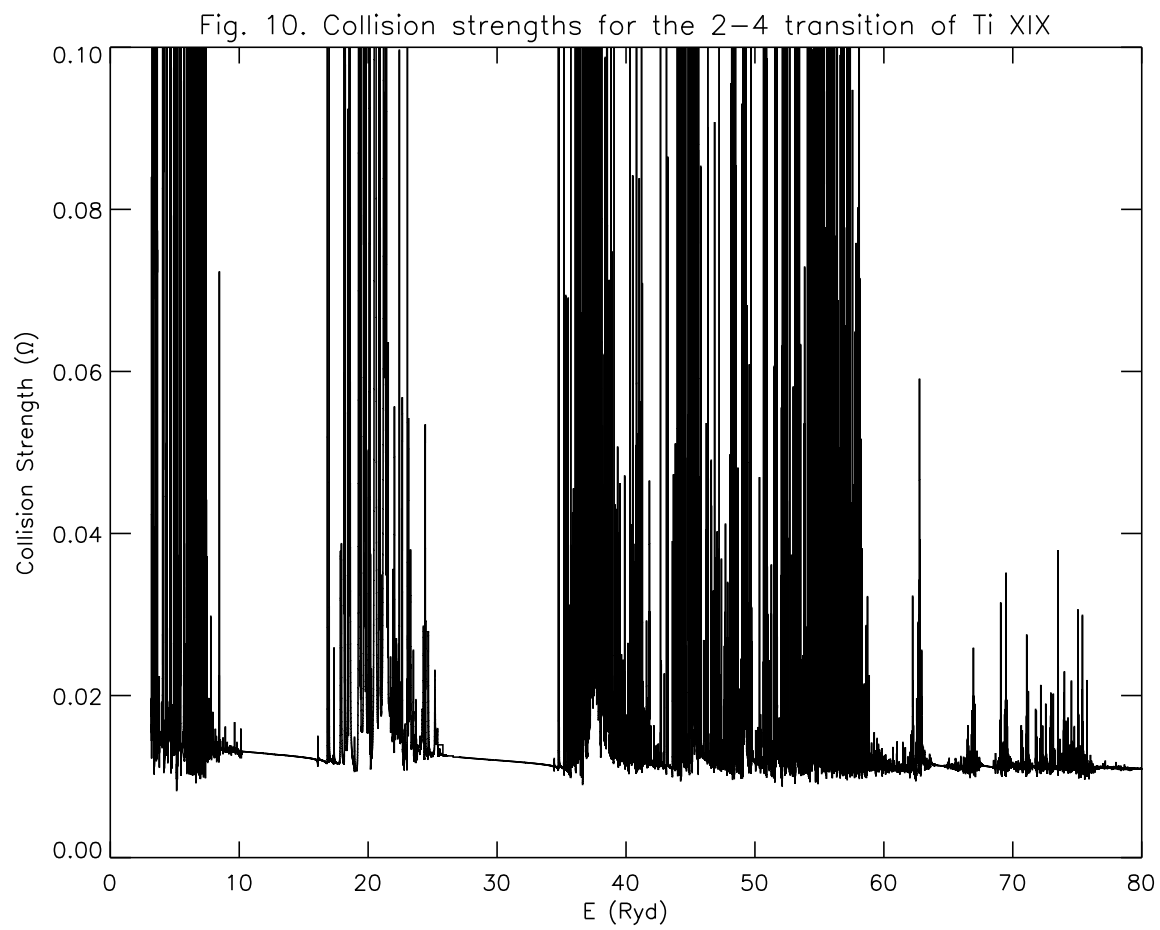


Figure 10: Collision strengths for the $2s2p\ ^3P_0 - 2s2p\ ^3P_2$ (2–4) transition of Ti XIX.

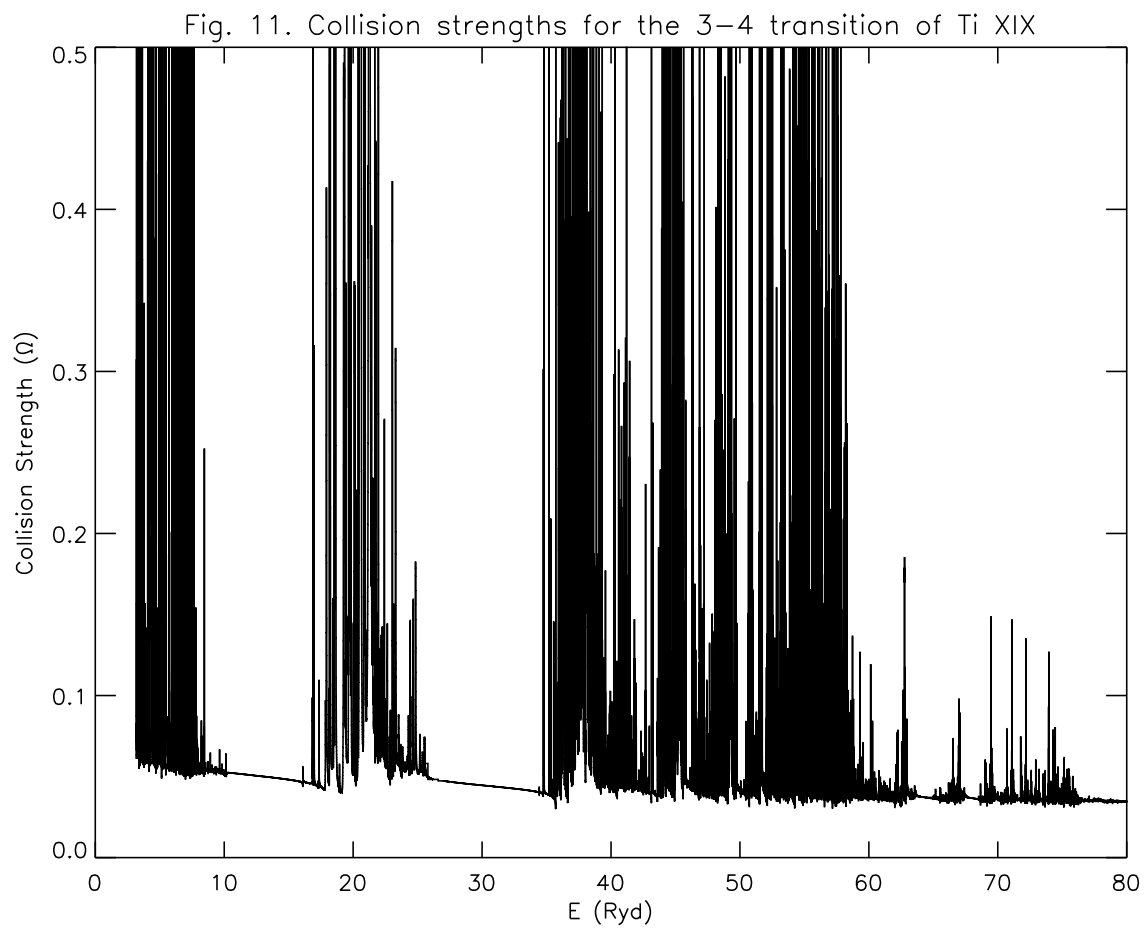


Figure 11: Collision strengths for the $2s2p\ ^3P_1^o - 2s2p\ ^3P_2^o$ (3–4) transition of Ti XIX.

Table 1: Energy levels (in Ryd) of Ti XIX and their lifetimes (τ , s). $a \pm b \equiv a \times 10^{\pm b}$.

Index	Configuration	Level	NIST	GRASP1	GRASP2	FAC1	FAC2	τ (s ⁻¹)
1	2s ²	¹ S ₀	0.00000	0.00000	0.00000	0.00000	0.00000
2	2s2p	³ P ₀ ^o	2.62618	2.62268	2.63105	2.63967	2.63907
3	2s2p	³ P ₁ ^o	2.77590	2.78404	2.78119	2.78920	2.78859	7.450-08
4	2s2p	³ P ₂ ^o	3.16447	3.18796	3.16788	3.17463	3.17411	9.798-04
5	2s2p	¹ P ₁ ^o	5.37367	5.46387	5.45302	5.45146	5.44666	7.155-11
6	2p ²	³ P ₀	7.06970	7.10469	7.10937	7.12758	7.12669	1.040-10
7	2p ²	³ P ₁	7.33470	7.37764	7.37028	7.38761	7.38685	9.398-11
8	2p ²	³ P ₂	7.58548	7.65312	7.62549	7.64194	7.64085	9.595-11
9	2p ²	¹ D ₂	8.36160	8.46555	8.43606	8.45099	8.44729	2.281-10
10	2p ²	¹ S ₀	10.06194	10.20533	10.19858	10.20719	10.20455	4.510-11
11	2s3s	³ S ₁	56.14134	56.22065	56.18639	56.18510	56.18496	5.249-13
12	2s3s	¹ S ₀		56.72694	56.69454	56.70758	56.70737	1.471-12
13	2s3p	³ P ₁ ^o	57.43898	57.45953	57.42614	57.43735	57.43687	3.601-13
14	2s3p	³ P ₀ ^o		57.46676	57.43697	57.44853	57.44867	3.773-11
15	2s3p	¹ P ₁ ^o		57.59804	57.55941	57.57007	57.56953	3.042-13
16	2s3p	³ P ₂ ^o		57.62728	57.58931	57.59959	57.59974	2.674-11
17	2s3d	³ D ₁	58.14431	58.29311	58.25119	58.26517	58.26290	9.053-14
18	2s3d	³ D ₂	58.22267	58.31519	58.27088	58.28462	58.28231	9.184-14
19	2s3d	³ D ₃	58.34570	58.34899	58.30331	58.31672	58.31437	9.354-14
20	2s3d	¹ D ₂	58.73936	58.84337	58.80058	58.81335	58.80922	1.310-13
21	2p3s	³ P ₀ ^o		59.52609	59.49725	59.52364	59.52383	7.179-13
22	2p3s	³ P ₁ ^o		59.63458	59.60204	59.62881	59.62857	6.572-13
23	2p3s	³ P ₂ ^o		60.10117	60.04739	60.07168	60.07186	6.185-13
24	2p3p	³ D ₁		60.35157	60.32192	60.34961	60.34956	4.444-13
25	2p3s	¹ P ₁ ^o		60.50059	60.45115	60.48131	60.47781	5.018-13
26	2p3p	³ D ₂	60.66305	60.69920	60.65945	60.68657	60.68621	5.143-13
27	2p3p	¹ P ₁	60.66305	60.70962	60.67058	60.69893	60.69880	3.752-13
28	2p3p	³ P ₀	60.92549	60.97659	60.94744	60.99706	60.99525	3.291-13
29	2p3p	³ D ₃	61.05216	61.12956	61.06979	61.09317	61.09299	5.181-13
30	2p3p	³ P ₁		61.15874	61.10785	61.13882	61.13841	3.461-13
31	2p3d	³ F ₂ ^o		61.17654	61.13912	61.17442	61.17252	8.358-13
32	2p3p	³ S ₁	61.06674	61.33556	61.28482	61.32152	61.32070	3.430-13
33	2p3p	³ P ₂		61.39848	61.34579	61.39096	61.38959	3.161-13
34	2p3d	³ F ₃ ^o		61.40858	61.36396	61.40354	61.40123	5.417-13
35	2p3d	¹ D ₂ ^o	61.40117	61.51326	61.46906	61.50920	61.50879	1.588-13
36	2p3d	³ D ₁ ^o	61.58343	61.70601	61.66333	61.70124	61.70128	7.765-14
37	2p3p	¹ D ₂	61.70098	61.79050	61.73569	61.78649	61.78290	2.429-13
38	2p3d	³ F ₄ ^o		61.79095	61.72657	61.76010	61.75762	1.967-10
39	2p3d	³ D ₂ ^o	61.86683	61.92348	61.86548	61.90434	61.90414	1.099-13
40	2p3d	³ D ₃ ^o	62.03542	62.09265	62.02908	62.06790	62.06775	7.894-14
41	2p3d	³ P ₂ ^o	62.09100	62.22337	62.16055	62.19689	62.19686	1.048-13
42	2p3d	³ P ₁ ^o	62.09100	62.24732	62.18674	62.22404	62.22392	1.151-13
43	2p3d	³ P ₀ ^o		62.26794	62.21350	62.25042	62.25021	1.319-13
44	2p3p	¹ S ₀		62.40839	62.36301	62.41988	62.40815	3.455-13
45	2p3d	¹ F ₃ ^o	62.61954	62.71188	62.64738	62.68766	62.68128	5.713-14
46	2p3d	¹ P ₁ ^o	62.56760	62.77356	62.71547	62.75247	62.75037	9.437-14

Table 1: Energy levels (in Ryd) of Ti XIX and their lifetimes (τ , s). $a \pm b \equiv a \times 10^{\pm b}$.

Index	Configuration	Level	NIST	GRASP1	GRASP2	FAC1	FAC2	τ (s ⁻¹)
47	2s4s	³ S ₁		75.38981	75.34908	75.35360	75.35248	9.907-13
48	2s4s	¹ S ₀		75.56940	75.52980	75.53766	75.53503	1.225-12
49	2s4p	³ P ₀ ^o		75.87605	75.83721	75.84719	75.84729	2.295-12
50	2s4p	³ P ₁ ^o		75.88694	75.84697	75.85715	75.85692	1.260-12
51	2s4p	³ P ₂ ^o		75.94341	75.90115	75.91045	75.91059	2.368-12
52	2s4p	¹ P ₁ ^o	75.87574	75.98058	75.93788	75.94922	75.94696	3.389-13
53	2s4d	³ D ₁	76.24025	76.21957	76.17599	76.18372	76.18259	2.312-13
54	2s4d	³ D ₂	76.20562	76.22736	76.18294	76.19065	76.18951	2.328-13
55	2s4d	³ D ₃	76.18284	76.24023	76.19533	76.20300	76.20187	2.351-13
56	2s4d	¹ D ₂		76.39832	76.35435	76.36012	76.35793	2.616-13
57	2s4f	³ F ₂ ^o		76.41805	76.37418	76.38062	76.37811	5.349-13
58	2s4f	³ F ₃ ^o		76.42175	76.37711	76.38354	76.38100	5.353-13
59	2s4f	³ F ₄ ^o		76.42768	76.38273	76.38910	76.38654	5.359-13
60	2s4f	¹ F ₃ ^o		76.46613	76.42163	76.42907	76.42635	5.456-13
61	2p4s	³ P ₀ ^o		78.45500	78.41892	78.44767	78.44781	1.199-12
62	2p4s	³ P ₁ ^o		78.49239	78.45542	78.48484	78.48335	1.034-12
63	2p4p	³ D ₁		78.81310	78.77651	78.80826	78.80833	5.671-13
64	2p4p	³ P ₁		78.97047	78.93198	78.96632	78.96487	5.426-13
65	2p4p	³ D ₂		78.97802	78.93780	78.97186	78.97107	5.830-13
66	2p4s	³ P ₂ ^o		79.03315	78.97319	78.99945	78.99966	8.714-13
67	2p4p	³ P ₀		79.04384	79.00783	79.04921	79.04442	5.681-13
68	2p4s	¹ P ₁ ^o		79.12885	79.06882	79.09698	79.09180	8.234-13
69	2p4d	³ F ₂ ^o		79.15188	79.11203	79.14333	79.14216	7.316-13
70	2p4d	³ F ₃ ^o		79.27787	79.23583	79.26668	79.26493	3.510-13
71	2p4d	³ D ₂ ^o		79.28651	79.24524	79.27575	79.27499	2.728-13
72	2p4d	³ D ₁ ^o		79.34204	79.30120	79.33063	79.32966	1.920-13
73	2p4f	³ G ₃		79.37004	79.32910	79.35644	79.35351	5.400-13
74	2p4f	³ F ₂		79.39082	79.34979	79.37766	79.37785	5.433-13
75	2p4f	³ F ₃		79.39114	79.35006	79.37781	79.37792	5.395-13
76	2p4f	³ G ₄		79.39525	79.35418	79.38193	79.37885	5.535-13
77	2p4p	¹ P ₁		79.45185	79.39094	79.42149	79.42107	5.108-13
78	2p4p	³ D ₃	79.36954	79.47881	79.41565	79.44415	79.44431	6.212-13
79	2p4p	³ P ₂		79.52313	79.46271	79.49773	79.49632	5.502-13
80	2p4p	³ S ₁		79.53841	79.47775	79.51011	79.50674	5.276-13
81	2p4p	¹ D ₂		79.67783	79.61622	79.65479	79.65120	4.909-13
82	2p4d	³ F ₄ ^o		79.75433	79.68940	79.71828	79.71673	1.088-12
83	2p4d	¹ D ₂ ^o	79.70306	79.76625	79.70271	79.73117	79.73051	3.384-13
84	2p4d	³ D ₃ ^o		79.82750	79.76291	79.79074	79.79028	2.260-13
85	2p4d	³ P ₂ ^o	79.46887	79.88056	79.81625	79.84389	79.84298	2.290-13
86	2p4d	³ P ₁ ^o		79.88919	79.82568	79.85354	79.85212	2.431-13
87	2p4d	³ P ₀ ^o		79.89819	79.83705	79.86505	79.86304	2.797-13
88	2p4p	¹ S ₀		79.90379	79.84573	79.89239	79.88819	6.549-13

Table 1: Energy levels (in Ryd) of Ti XIX and their lifetimes (τ , s). $a\pm b \equiv a\times 10^{\pm b}$.

Index	Configuration	Level	NIST	GRASP1	GRASP2	FAC1	FAC2	τ (s^{-1})
89	2p4f	1F_3		79.92931	79.86466	79.88954	79.86857	5.386-13
90	2p4f	3F_4		79.94410	79.87919	79.90411	79.90253	5.439-13
91	2p4f	3D_3		79.97863	79.91434	79.93935	79.93950	5.380-13
92	2p4f	3D_2		79.98128	79.91719	79.94263	79.94099	5.385-13
93	2p4f	3G_5		79.98694	79.92135	79.94597	79.94267	5.429-13
94	2p4f	1G_4		80.00956	79.94390	79.96957	79.96434	5.681-13
95	2p4f	3D_1		80.03020	79.96676	79.99200	79.99212	5.353-13
96	2p4d	$^1F_3^o$	79.96824	80.04175	79.97704	80.00288	79.99691	1.416-13
97	2p4f	1D_2		80.05501	79.99117	80.01690	80.01675	5.388-13
98	2p4d	$^1P_1^o$		80.07038	80.00818	80.03399	80.02969	2.077-13

NIST: <http://nist.gov/pml/data/asd.cfm>

GRASP1: Energies from the GRASP code with 98 level calculations *without* Breit and QED effects

GRASP2: Energies from the GRASP code with 98 level calculations *with* Breit and QED effects

FAC1: Energies from the FAC code with 98 level calculations

FAC2: Energies from the FAC code with 166 level calculations

Table 3: Comparison between GRASP and FAC A- values (s^{-1}) for some transitions of Ti XIX. ($a\pm b \equiv a \times 10^{\pm b}$).

i	j	f (GRASP)	A (GRASP)	A (FAC)	A(GRASP)/A(FAC)
1	3	6.4812-04	1.3423+07	1.359+07	0.99
1	5	1.7554-01	1.3976+10	1.395+10	1.00
1	13	3.0051-01	2.6535+12	2.704+12	0.98
1	15	3.5360-01	3.1367+12	3.139+12	1.00
2	7	6.9804-02	4.1978+09	4.216+09	1.00
2	11	2.7373-02	2.1021+11	2.138+11	0.98
2	17	7.4379-01	6.1609+12	6.164+12	1.00
3	7	1.6691-02	2.8235+09	2.836+09	1.00
3	8	2.9978-02	3.3905+09	3.406+09	1.00
3	9	7.9155-04	1.2199+08	1.216+08	1.00
3	10	5.0895-05	6.7477+07	6.728+07	1.00
3	11	2.7504-02	6.3011+11	6.398+11	0.98
3	12	3.2644-05	2.2865+09	2.542+09	0.90
3	17	1.8421-01	4.5527+12	4.552+12	1.00
3	18	5.5139-01	8.1824+12	8.191+12	1.00
3	20	1.3291-03	2.0101+10	2.005+10	1.00
4	7	1.5298-02	3.6169+09	3.639+09	0.99
4	8	4.3448-02	6.9346+09	6.970+09	0.99
4	9	6.6129-03	1.4742+09	1.481+09	1.00
4	11	2.8159-02	1.0597+12	1.073+12	0.99
4	17	7.3864-03	3.0003+11	2.995+11	1.00
4	18	1.1007-01	2.6845+12	2.684+12	1.00
4	19	6.1290-01	1.0690+13	1.071+13	1.00
4	20	1.2753-04	3.1706+09	3.292+09	0.96
5	6	1.5967-04	1.0556+07	1.086+07	0.97
5	7	6.2606-05	1.8485+06	1.906+06	0.97
5	8	4.2613-03	9.6929+07	9.917+07	0.98
5	9	6.5004-02	2.7878+09	2.832+09	0.98
5	10	4.0732-02	2.2105+10	2.220+10	1.00
5	11	2.4577-04	5.0813+09	5.156+09	0.99
5	12	1.0706-02	6.7738+11	6.918+11	0.98
5	17	1.4504-03	3.2478+10	3.240+10	1.00
5	18	1.6119-03	2.1672+10	2.255+10	0.96
5	20	5.5415-01	7.6008+12	7.577+12	1.00
6	13	6.4543-04	4.3753+09	4.612+09	0.95
6	15	8.4843-04	5.7819+09	5.845+09	0.99
7	13	1.9886-04	4.0023+09	4.093+09	0.98
7	14	3.9853-04	2.4073+10	2.495+10	0.96
7	15	7.6560-05	1.5491+09	1.648+09	0.94
7	16	9.2907-04	1.1292+10	1.149+10	0.98
8	13	1.1242-03	3.7325+10	3.847+10	0.97
8	15	1.7751-04	5.9255+09	5.804+09	1.02
8	16	1.0792-03	2.1640+10	2.213+10	0.98
9	13	2.1883-03	7.0310+10	7.267+10	0.97
9	15	4.0870-03	1.3203+11	1.333+11	0.99
9	16	8.8457-05	1.7167+09	1.798+09	0.95
10	13	9.6368-04	5.7551+09	5.311+09	1.08

Table 4: Collision strengths for resonance transitions of Ti XIX. ($a\pm b \equiv a \times 10^{\pm b}$).

Transition		Energy (Ryd)						
i	j	100	300	500	700	900	1100	FAC ^c
1	2	7.561-4	2.120-4	9.758-5	5.602-5	3.634-5	2.552-5	6.199-5
1	3	8.260-3	6.955-3	6.406-3	5.839-3	5.803-3	5.396-3	8.643-3
1	4	3.693-3	1.029-3	4.723-4	2.708-4	1.755-4	1.232-4	3.004-4
1	5	6.500-1	7.992-1	8.038-1	7.428-1	7.618-1	6.805-1	9.797-1
1	6	7.543-5	5.139-5	4.662-5	4.490-5	4.415-5	4.381-5	3.522-5
1	7	6.142-5	1.110-5	3.823-6	1.763-6	9.633-7	5.860-7	2.136-6
1	8	3.899-4	3.753-4	3.855-4	3.946-4	4.008-4	4.053-4	3.794-4
1	9	1.956-3	2.251-3	2.366-3	2.436-3	2.480-3	2.510-3	2.516-3
1	10	9.304-4	7.814-4	7.271-4	7.010-4	6.867-4	6.788-4	6.010-4
1	11	7.696-4	1.533-4	6.489-5	3.589-5	2.281-5	1.587-5	3.429-5
1	12	2.021-2	2.373-2	2.471-2	2.526-2	2.568-2	2.605-2	2.502-2
1	13	9.225-3	2.333-2	3.210-2	3.855-2	4.390-2	4.737-2	4.099-2
1	14	2.251-4	3.678-5	1.397-5	7.212-6	4.372-6	2.925-6	6.113-6
1	15	1.093-2	2.841-2	3.923-2	4.718-2	5.381-2	5.802-2	4.675-2
1	16	1.107-3	1.807-4	6.856-5	3.537-5	2.143-5	1.433-5	3.005-5
1	17	1.212-3	2.005-4	7.732-5	4.038-5	2.466-5	1.659-5	3.809-5
1	18	2.070-3	4.163-4	2.215-4	1.651-4	1.422-4	1.304-4	1.726-4
1	19	2.835-3	4.686-4	1.807-4	9.434-5	5.761-5	3.874-5	8.936-5
1	20	3.295-2	5.466-2	6.168-2	6.518-2	6.732-2	6.843-2	6.551-2
1	21	3.380-6	6.468-7	2.543-7	1.332-7	8.108-8	5.445-8	1.309-7
1	22	2.104-4	5.242-4	7.223-4	8.692-4	9.903-4	1.068-3	8.388-4
1	23	1.464-5	2.855-6	1.129-6	5.942-7	3.637-7	2.453-7	5.739-7
1	24	3.916-5	9.693-6	4.779-6	3.012-6	2.147-6	1.648-6	1.402-6
1	25	7.582-4	1.930-3	2.663-3	3.208-3	3.655-3	3.945-3	3.425-3
1	26	8.262-5	5.163-5	4.967-5	4.994-5	5.051-5	5.094-5	4.393-5
1	27	2.660-5	7.211-6	3.857-6	2.572-6	1.907-6	1.506-6	8.167-7
1	28	1.064-5	6.978-6	6.648-6	6.608-6	6.627-6	6.671-6	6.480-6
1	29	6.875-5	1.412-5	5.666-6	2.985-6	1.824-6	1.226-6	3.074-6
1	30	1.825-5	4.900-6	2.644-6	1.778-6	1.326-6	1.052-6	5.392-7
1	31	4.376-5	7.752-6	4.091-6	2.927-6	2.353-6	2.004-6	8.870-7
1	32	1.424-5	2.587-6	1.006-6	5.299-7	3.279-7	2.233-7	4.067-7
1	33	6.018-5	7.790-5	8.599-5	9.012-5	9.268-5	9.422-5	8.231-5
1	34	6.250-5	2.166-5	1.869-5	1.832-5	1.843-5	1.863-5	1.714-5
1	35	4.534-5	1.091-5	7.120-6	5.685-6	4.861-6	4.298-6	8.240-7
1	36	2.527-4	4.217-4	5.235-4	5.984-4	6.596-4	6.996-4	5.493-4
1	37	1.927-4	3.241-4	3.639-4	3.824-4	3.933-4	3.999-4	3.693-4
1	38	6.185-5	8.327-6	3.009-6	1.534-6	9.289-7	6.233-7	1.475-6
1	39	3.274-5	7.004-6	4.295-6	3.339-6	2.817-6	2.472-6	6.715-7
1	40	2.451-5	8.938-6	8.289-6	8.386-6	8.565-6	8.732-6	8.455-6
1	41	5.272-5	8.133-6	3.189-6	1.742-6	1.127-6	8.066-7	1.496-6
1	42	5.086-5	2.868-5	3.061-5	3.360-5	3.646-5	3.838-5	3.233-5
1	43	1.476-5	2.298-6	8.707-7	4.513-7	2.749-7	1.847-7	4.387-7
1	44	7.843-5	7.521-5	7.541-5	7.593-5	7.651-5	7.717-5	7.792-5
1	45	1.622-4	2.208-4	2.399-4	2.514-4	2.598-4	2.661-4	2.609-4
1	46	1.534-3	2.721-3	3.392-3	3.883-3	4.283-3	4.545-3	3.815-3
1	47	3.390-4	5.704-5	2.317-5	1.257-5	7.906-6	5.458-6	1.158-5
1	48	3.738-3	4.659-3	4.909-3	5.042-3	5.141-3	5.224-3	5.034-3

Table 4: Collision strengths for resonance transitions of Ti XIX. ($a \pm b \equiv a \times 10^{\pm b}$).

Transition		Energy (Ryd)						
i	j	100	300	500	700	900	1100	FAC ^c
1	50	7.954-4	1.383-3	1.864-3	2.225-3	2.518-3	2.725-3	2.222-3
1	51	5.696-4	7.775-5	2.792-5	1.400-5	8.344-6	5.504-6	1.215-5
1	52	3.309-3	9.083-3	1.257-2	1.510-2	1.714-2	1.857-2	1.605-2
1	53	4.978-4	7.552-5	2.857-5	1.479-5	8.990-6	6.024-6	1.368-5
1	54	8.401-4	1.491-4	7.445-5	5.322-5	4.463-5	4.044-5	5.443-5
1	55	1.159-3	1.755-4	6.635-5	3.434-5	2.087-5	1.398-5	3.184-5
1	56	4.843-3	8.628-3	9.829-3	1.043-2	1.080-2	1.107-2	1.041-2
1	57	3.353-4	3.186-5	1.033-5	4.982-6	2.916-6	1.912-6	3.461-6
1	58	4.825-4	7.648-5	4.932-5	4.302-5	4.087-5	3.994-5	4.698-5
1	59	6.019-4	5.701-5	1.847-5	8.903-6	5.210-6	3.415-6	6.229-6
1	60	1.852-3	3.257-3	3.517-3	3.625-3	3.695-3	3.740-3	3.690-3
1	61	1.741-6	2.816-7	1.075-7	5.568-8	3.380-8	2.270-8	5.087-8
1	62	1.517-5	2.126-5	2.699-5	3.128-5	3.471-5	3.716-5	3.363-5
1	63	1.141-5	2.149-6	9.625-7	5.794-7	4.035-7	3.057-7	3.043-7
1	64	1.037-5	1.796-6	7.751-7	4.567-7	3.133-7	2.346-7	2.541-7
1	65	1.695-5	6.359-6	5.579-6	5.471-6	5.474-6	5.504-6	4.351-6
1	66	8.556-6	1.488-6	5.866-7	3.121-7	1.941-7	1.334-7	2.671-7
1	67	1.226-5	1.172-5	1.217-5	1.253-5	1.281-5	1.304-5	1.281-5
1	68	2.337-5	3.711-5	4.731-5	5.476-5	6.065-5	6.490-5	6.279-5
1	69	2.101-5	2.810-6	1.192-6	7.345-7	5.347-7	4.251-7	3.531-7
1	70	2.613-5	8.765-6	8.074-6	8.204-6	8.426-6	8.649-6	9.531-6
1	71	2.543-5	3.428-6	1.414-6	8.473-7	6.038-7	4.728-7	4.439-7
1	72	1.141-4	1.961-4	2.440-4	2.789-4	3.070-4	3.283-4	2.627-4
1	73	5.650-6	6.905-7	3.457-7	2.324-7	1.760-7	1.422-7	5.481-8
1	74	1.637-5	3.022-5	3.640-5	3.971-5	4.181-5	4.303-5	3.912-5
1	75	8.302-6	8.702-7	3.611-7	2.189-7	1.561-7	1.213-7	9.118-8
1	76	7.436-6	5.314-6	5.892-6	6.290-6	6.571-6	6.783-6	6.587-6
1	77	7.309-6	1.609-6	8.850-7	6.179-7	4.774-7	3.899-7	1.226-7
1	78	1.970-5	3.296-6	1.250-6	6.409-7	3.857-7	2.564-7	6.115-7
1	79	1.043-5	4.104-6	3.713-6	3.674-6	3.686-6	3.709-6	2.854-6
1	80	9.624-6	1.660-6	6.735-7	3.697-7	2.370-7	1.666-7	2.799-7
1	81	1.139-5	1.229-5	1.346-5	1.398-5	1.425-5	1.441-5	1.076-5
1	82	2.942-5	3.510-6	1.230-6	6.184-7	3.715-7	2.479-7	5.861-7
1	83	1.420-5	2.497-6	1.425-6	1.075-6	8.928-7	7.763-7	1.597-7
1	84	1.372-5	2.257-6	1.527-6	1.404-6	1.387-6	1.398-6	1.726-6
1	85	2.228-5	2.877-6	1.054-6	5.535-7	3.482-7	2.442-7	4.555-7
1	86	1.965-5	7.175-6	6.954-6	7.432-6	7.973-6	8.430-6	7.865-6
1	87	7.132-6	9.664-7	3.505-7	1.777-7	1.067-7	7.100-8	1.625-7
1	88	4.233-5	4.621-5	4.867-5	5.026-5	5.148-5	5.247-5	5.448-5
1	89	3.541-6	6.445-7	4.000-7	2.992-7	2.411-7	2.029-7	2.712-8
1	90	3.440-6	6.498-7	5.698-7	5.732-7	5.854-7	5.978-7	5.785-7
1	91	6.938-6	7.258-7	3.153-7	1.995-7	1.469-7	1.171-7	5.622-8
1	92	1.004-5	1.510-5	1.812-5	1.981-5	2.091-5	2.153-5	2.033-5
1	93	7.123-6	6.086-7	2.188-7	1.130-7	6.895-8	4.640-8	8.223-8
1	94	8.379-6	9.444-6	1.072-5	1.150-5	1.203-5	1.243-5	1.245-5
1	95	4.414-6	3.638-7	1.129-7	5.313-8	3.059-8	1.982-8	3.719-8
1	96	2.170-5	2.570-5	2.883-5	3.082-5	3.226-5	3.341-5	4.402-5

Table 6: Comparison of Υ values for transitions of Ti XIX. ($a \pm b \equiv a \times 10^{\pm b}$).

log T_e (K)		6.3			6.9			7.5		
i	j	DARC	FAC	ZS	DARC	FAC	ZS	DARC	FAC	ZS
1	2	3.550-3	1.693-3	1.7943-3	2.753-3	1.242-3	1.3135-3	1.240-3	6.553-4	6.9065-4
1	3	1.480-2	8.981-3	9.1369-3	1.326-2	8.517-3	8.6113-3	9.330-3	8.208-3	8.1786-3
1	4	2.041-2	8.224-3	8.7866-3	1.497-2	6.031-3	6.4270-3	6.568-3	3.180-3	3.3795-3
1	5	4.632-1	4.683-1	4.4407-1	5.414-1	5.558-1	5.4721-1	6.535-1	7.149-1	7.1229-1
1	6	2.607-4	1.126-4	1.1731-4	2.678-4	8.760-5	8.9602-5	1.421-4	6.029-5	5.9662-5
1	7	5.441-4	2.059-4	2.2788-4	5.371-4	1.369-4	1.5205-4	2.272-4	6.298-5	6.7922-5
1	8	1.003-3	5.224-4	4.8162-4	1.002-3	4.565-4	3.9854-4	6.263-4	4.007-4	3.2024-4
1	9	2.566-3	1.645-3	1.2143-3	2.660-3	1.826-3	1.3591-3	2.379-3	2.116-3	1.5968-3
1	10	1.537-3	6.803-4	5.7142-4	1.550-3	6.579-4	5.5271-4	1.102-3	6.290-4	5.3012-4
2	3	4.162-2	1.801-2	1.9718-2	2.591-2	1.262-2	1.3622-2	1.118-2	6.353-3	6.8570-3
2	4	3.037-2	1.380-2	1.3591-2	2.181-2	1.266-2	1.2352-2	1.490-2	1.192-2	1.1670-2
2	5	9.787-3	4.090-3	4.4369-3	8.125-3	2.829-3	3.0501-3	3.445-3	1.387-3	1.4701-3
2	6	2.106-3	1.079-3	1.1455-3	1.733-3	7.869-4	8.3760-4	7.891-4	4.119-4	4.3712-4
2	7	2.202-1	2.226-1	2.2221-1	2.571-1	2.651-1	2.7186-1	3.058-1	3.409-1	3.4776-1
2	8	5.388-3	2.428-3	2.5623-3	4.697-3	1.774-3	1.8632-3	2.101-3	9.312-4	9.7530-4
2	9	3.211-3	1.243-3	1.3231-3	2.916-3	9.069-4	9.6379-4	1.262-3	4.755-4	5.0398-4
2	10	5.646-4	1.509-4	1.5738-4	4.844-4	1.072-4	1.1212-4	1.976-4	5.397-5	5.6180-5
3	4	1.550-1	5.275-2	5.4204-2	9.090-2	4.364-2	4.4300-2	4.970-2	3.436-2	3.4175-2
3	5	3.741-2	1.261-2	1.3622-2	2.691-2	8.896-3	9.5108-3	1.147-2	4.685-3	4.9728-3
3	6	2.262-1	2.282-1	2.2576-1	2.631-1	2.725-1	2.7867-1	3.112-1	3.505-1	3.5752-1
3	7	1.729-1	1.702-1	1.6936-1	1.991-1	2.011-1	2.0605-1	2.307-1	2.564-1	2.6172-1
3	8	2.864-1	2.836-1	2.8422-1	3.313-1	3.355-1	3.4509-1	3.849-1	4.288-1	4.3893-1
3	9	1.843-2	1.106-2	1.0630-2	1.805-2	1.082-2	1.0263-2	1.354-2	1.111-2	1.0400-2
3	10	2.511-3	8.760-4	9.0560-4	2.237-3	7.512-4	7.8159-4	1.196-3	6.309-4	6.5237-4
4	5	7.273-2	2.146-2	2.3186-2	4.562-2	1.488-2	1.6003-2	1.844-2	7.398-3	7.8110-3
4	6	3.254-3	8.655-4	9.4764-4	2.512-3	6.355-4	6.9369-4	1.052-3	3.358-4	3.6439-4
4	7	2.884-1	2.858-1	2.8227-1	3.333-1	3.407-1	3.4819-1	3.890-1	4.371-1	4.4551-1
4	8	7.430-1	7.522-1	7.5185-1	8.635-1	8.957-1	9.2247-1	1.014+0	1.150+0	1.1785+0
4	9	1.280-1	1.069-1	1.0317-1	1.393-1	1.202-1	1.1693-1	1.469-1	1.465-1	1.4356-1
4	10	6.400-3	1.849-3	1.9425-3	5.279-3	1.328-3	1.3970-3	2.164-3	6.808-4	7.1247-4
5	6	9.319-3	6.618-3	7.2781-3	9.312-3	7.599-3	8.5691-3	8.387-3	9.108-3	1.0238-2
5	7	1.407-2	5.982-3	6.2057-3	1.208-2	5.274-3	5.4767-3	6.677-3	4.463-3	4.6440-3
5	8	1.270-1	1.116-1	1.1022-1	1.378-1	1.338-1	1.3584-1	1.462-1	1.687-1	1.7047-1
5	9	1.074+0	1.094+0	1.0744+0	1.237+0	1.328+0	1.3820+0	1.422+0	1.717+0	1.7953+0
5	10	3.799-1	3.868-1	3.9823-1	4.431-1	4.613-1	4.8814-1	5.268-1	5.939-1	6.2552-1
6	7	3.074-2	1.923-2	2.0870-2	2.496-2	1.359-2	1.4672-2	1.144-2	6.908-3	7.3534-3
6	8	2.441-2	1.730-2	1.7613-2	2.226-2	1.526-2	1.5500-2	1.620-2	1.347-2	1.3428-2
6	9	1.137-2	6.189-3	6.9335-3	9.442-3	4.247-3	4.7452-3	4.080-3	2.062-3	2.2528-3
6	10	3.660-3	9.244-4	1.0278-3	3.010-3	6.115-4	6.7632-4	1.169-3	2.795-4	3.0982-4
7	8	8.444-2	5.652-2	5.9629-2	7.490-2	4.555-2	4.7635-2	4.542-2	3.381-2	3.4716-2
7	9	5.030-2	2.925-2	3.1902-2	4.358-2	2.095-2	2.2555-2	2.079-2	1.163-2	1.2341-2
7	10	1.383-2	3.944-3		1.088-2	2.632-3		4.220-3	1.221-3	
8	9	1.013-1	6.637-2	7.0516-2	8.985-2	5.088-2	5.3039-2	5.028-2	3.388-2	3.3996-2
8	10	1.998-2	8.238-3	8.7911-3	1.620-2	6.240-3	6.4961-3	7.948-3	4.246-3	4.2710-3
9	10	3.972-2	2.929-2	2.8800-2	4.004-2	3.092-2	3.0604-2	3.769-2	3.457-2	3.4692-2